Space-Time Wireless Systems: From Array Processing to MIMO Communications

Edited by

H. Bölcskei, D. Gesbert, C. Papadias, and A. J. van der Veen

Contents

Part I

Multiantenna basics

5

The role of feedback, CSI, and coherence in MIMO systems

G. Barriac, N. Jacobsen, and U. Madhow

Department of Electrical and Computer Engineering
University of California, Santa Barbara

5.1 Introduction

The growth in wireless communication over the past decade has been fueled by the demand for high-speed wireless data, in addition to the basic cellular telephony service which is now an indispensable part of our lives. Cellular operators are upgrading their networks to support higher data rates, and the imminent completion of the 802.16 and 802.20 standards is precipitating the move towards ubiquitous broadband wireless access. Increasing the capacity of current wireless links is perhaps the most essential step in realizing the vision of high-speed wireless data on demand, and adding multiple antennas at both the transmitter and the receiver is known to dramatically increase capacity. In this chapter, we explore the role of channel knowledge at the transmitter in Multiple-Input Multiple-Output (MIMO) systems. While feedback produces marginal gains in single antenna communication, even partial channel knowledge at the transmitter is known to produce large performance gains in MIMO systems. We also consider the benefits of partial channel knowledge at the receiver in noncoherent systems.

For indoor Wireless Local Area Network (WLAN) systems with MIMO capabilities, such as the Bell Labs BLAST prototype and emerging 802.11n standards efforts, the system bandwidth is typically within the channel coherence bandwidth, which is large because of small indoor delay spreads. On the other hand, emerging high-speed outdoor Wireless Metropolitan Area Network (WMAN) communication systems such as 802.16 and 802.20 can easily span a band which is several times the channel coherence bandwidth, which is smaller due to larger delay spreads in outdoor channels. Moreover, the angular spread in paths from transmitter to receiver in outdoor channels is often much smaller than for indoor channels, because of the typically high altitude of the base station. Thus, outdoor spatial channels have a relatively small number of dominant spatial modes, and can therefore benefit more from channel knowledge at the transmitter regarding these modes. Our emphasis in this chapter, therefore, is on outdoor communication systems, where implicit or explicit feedback regarding the channel is expected to be most effective. In particular, we show that certain types of Channel State Information (CSI) can be obtained robustly and without training overhead in wideband systems. Such "implicit" feedback is particularly useful for outdoor channels, where it leads to both large performance gains *and* simpler transceivers.

An important design consideration is the exploitation of the asymmetry inherent in outdoor cellular or fixed wireless applications, where the base station is significantly more capable than the subscriber unit. Specifically, the base station can potentially have a large number of antennas, whereas the subscriber unit may have no more than one or two, and the base station is capable of more complex signal processing. Thus, subscriber units with a single antenna lead to the important special cases of Multiple-Input, Single-Output (MISO) models for downlink communication, and Single-Input, Multiple-Output (SIMO) models for uplink communication. For concreteness, we focus on Orthogonal Frequency Division Multiplexing (OFDM), which has been designated as the physical layer in emerging outdoor WMAN standards such as 802.16a and 802.20, as well as indoor WLAN standards such as 802.11n. Our approach is to characterize information theoretic limits, with the understanding that rapid advances in turbo-like coded modulation have brought such limits within reach using relatively standard architectures.

5.1.1 Feedback in narrowband systems

When both transmitter and receiver have perfect knowledge of the channel, Telatar's seminal work (Telatar, 1995) shows that the capacity achieving transmit strategy is to send independent Gaussian symbols along the channel eigenvectors, with the power on each symbol being determined by the classical "waterfilling" solution. While the resulting capacity gains over single antenna channels are impressive (Telatar, 1995; Biglieri *et al.*, 2001), in practice, perfect channel knowledge is difficult to obtain.

Receiver CSI: In many scenarios, the transmitter can send sufficiently many training, or pilot, symbols such that the receiver can accurately estimate the channel. Hence, the approximation that the receiver has perfect CSI is often reasonable, especially for downlink communication, where a common pilot can be employed for channel estimation by a large number of subscribers. We revisit this standard assumption of *coherent* reception in

Section 5.4, which focuses on uplink communication, in which pilots cannot be shared and are therefore more expensive.

Transmitter CSI: The role of CSI at the transmitter is the main focus of this chapter. Two standard mechanisms for obtaining CSI at the transmitter are as follows.

(a) *Implicit feedback using reciprocity:* If the same frequency band is employed for both uplink and downlink, as in a Time Division Duplex (TDD) system, then the instantaneous channels for uplink and downlink are identical. Thus, estimates of the channel on the uplink can be employed for downlink transmission, and vice versa. Inaccuracy in such implicit feedback occurs because the channel may change between the time that the channel estimate is obtained, and the time when the resulting implicit feedback is employed.

(b) *Explicit feedback:* If the uplink and downlink employ different frequency bands, as in a Frequency Division Duplex (FDD) system, or if the implicit feedback due to reciprocity in a TDD system is unreliable due to channel time variations, then channel information can be sent back to the transmitter using explicit feedback. The challenge with this approach is the design of economical and robust explicit feedback mechanisms.

For a time-varying wireless channel, it is unrealistic to expect either of these two mechanisms to yield perfect CSI at the transmitter, so that it is important to design systems and evaluate their performance under the assumption of *partial* CSI. While CSI yields marginal performance gains for single antenna communication, for MIMO systems, even partial CSI is known to yield large potential performance gains (Narula *et al.*, 1998; Visotsky and Madhow, 2001; Medles *et al.*, 2003).

Research on improving the capacity of narrowband MIMO channels via a feedback channel to the transmitter include Lau *et al.* (2003); Jongren *et al.* (2002); Mukkavilli *et al.* (2003b). Lau *et al.* consider optimizing the CSI sent over a feedback channel, imposing a capacity constraint on the maximum number of bits sent per fading block. It is shown that the optimal feedback scheme is equivalent to the design of a vector quantizer with a modified distortion measure. Jongren *et al.* assume that quantized channel information is available at the transmitter, and employ it to guide the design of space-time block codes preceded by CSI dependent precoding matrices. Given the cost of sending back quantized channel values, many researchers have looked at scenarios where the receiver sends back information which designates the transmission strategy to be used. Mukkavilli *et al.* investigate outage in MISO channels using beamforming, where the beamforming vector is determined by a finite capacity feedback channel carrying the index of the desired beamformer. The construction of near-optimal beamformer codebooks for this purpose is considered in Mukkavilli *et al.* (2003a).

Beamforming to maximize the received Signal-to-Noise Ratio (SNR), using CSI obtained by *reciprocity*, is studied in Cavers (2002). It is shown that for outdoor urban models, the time between the uplink and downlink should be limited to 10 ms in order for the uplink measurements to be useful for capacity enhancement on the downlink.

For wireless mobile channels, second order channel statistics vary much more slowly than the channel realization itself. Thus, an important model for robust channel CSI at the transmitter is that of spatial *covariance feedback.* Information theoretic computations show that such covariance feedback greatly improves capacity when the spatial channel is strongly colored (Visotsky and Madhow, 2001; Jafar and Goldsmith, 2001; Jafar *et al.*, 2001). Visotsky and Madhow (2001) show that the optimal strategy for MISO systems with covariance feedback is a form of waterfilling, subject to a sum power constraint, along the eigenvectors of the covariance matrix. This result is extended to systems with multiple receive antennas by Jafar *et al.* (2001), modeling the channel responses for different receive antenna elements as uncorrelated. Efficient computation of the waterfilling solution is considered in Boche and Jorswieck (2003a,b); Simon and Moustakas (2002). The ergodic and outage capacity for narrowband MIMO channels with covariance feedback is considered in Kang and Alouini (2003). The waterfilling strategy with covariance feedback can be interpreted as a linear precoding matrix which directs energy along the eigenvectors, followed by a space-time or space-frequency code for diversity or multiplexing, with the eigendirections forming "virtual" antenna elements. Examples of constructive space-time coding schemes preceded by linear precoding based on covariance feedback include BLAST-like spatial multiplexing (Simeone and Spagnolini, 2003), and diversity using space-time block codes (Zhou and Giannakis, 2003). The results confirm the performance improvements from covariance feedback predicted by information-theoretic computations.

5.1.2 Feedback in wideband systems

OFDM provides a convenient method of decomposing a wideband channel into a collection of parallel narrowband channels, or subcarriers. In principle, therefore, narrowband space-time communication techniques can be applied on a per subcarrier basis in OFDM systems. However, obtaining and using channel feedback per subcarrier can be computationally complex, expensive in terms of training overhead, and sensitive to channel estimation errors.

Recent work on MIMO-OFDM systems with per-subcarrier channel feedback include Xia *et al.* (2004); Vook *et al.* (2003). In Xia *et al.* (2004), a feedback model is considered where the transmitter knows each subcarrier's channel up to a certain uncertainty. A precoder based on the available CSI is used with a space-time code on a per-subcarrier basis, and an adaptive power and bit loading scheme across subcarriers is also used. Vook *et al.* (2003) consider the performance of MIMO OFDM under various assumptions on the information available at the transmitter. This work reports on simulation-based results for specific code-constructions, and indicates a sensitivity to errors in the transmitter's CSI.

The performance of channel estimation and feedback can be improved by exploiting the high degree of correlation between channels on neighboring subcarriers. In particular, it can be shown (Barriac and Madhow, 2004a), that the channel spatial covariance is invariant across frequency. Thus, implicit feedback regarding the downlink covariance matrix can be obtained by suitably averaging uplink measurements, for both TDD and FDD systems (Barriac and Madhow, 2004b). This concept, which we term *statistical reciprocity,* is therefore more general than the deterministic reciprocity employed to obtain implicit feedback in TDD systems. The covariance feedback obtained from statistical reciprocity is robust, since it is invariant across frequency and varies very slowly with time. This is in contrast to the fragility of both implicit and explicit feedback regarding the channel realization per subcarrier, which varies relatively rapidly across both frequency and time. Implicit covariance feedback is particularly effective for outdoor channels for several reasons. First, accurate estimation of the covariance by averaging across frequency is possible because of the smaller coherence bandwidth. Second, covariance feedback is especially useful when the spatial covariance is strongly colored, as is typically the case for the narrow power-angle profiles seen in outdoor environments. Third, since the covariance is invariant across subcarriers, so is the space-time communication strategy based on covariance feedback, which significantly reduces transceiver complexity. For the remainder of this chapter, therefore, we focus on system designs centered around the "free" availability of the spatial covariance matrix at the base station in a cellular-like OFDM system.

The notion of using covariance information on the uplink to optimize downlink transmission has previously been applied in the context of frequency division duplex (FDD) systems using TDMA or DS-CDMA (Morgan, 2003; Hochwald and Marzetta, 2001; Liang and Chin, 2001; Raleigh and Jones, 1997). The covariance is obtained either by averaging uplink channel responses across *time*, or by estimating the directions of arrival (DOA) of the incoming paths, and directly determining the covariance from these measurements. DOA estimation is known to be computationally intensive (Liang and Chin, 2001), and may be infeasible if there are too many multipath components, or an insufficient number of antenna elements. On the other hand, time averaging has the disadvantage that the amount of time necessary to construct an accurate estimate of the covariance matrix may exceed the allotted uplink transmit time.

Statistical reciprocity applies directly for both TDD systems, and for FDD systems in which the uplink and downlink bands are close enough that the array response for a given DOA is approximately the same on both uplink and downlink. For FDD systems in which the uplink and downlink bands are widely separated, this assumption may break down. However, it is possible to transform the uplink covariance matrix to obtain the downlink covariance matrix using a frequency calibration matrix (Liang and Chin, 2001), or by use of a clever antenna configuration (Hochwald and Marzetta, 2001) that attains identical beampatterns at both uplink/downlink wavelengths. These techniques, originally developed for single-carrier systems, are directly applicable to OFDM systems as well.

5.1.3 Chapter organization

The remainder of this chapter is organized as follows. Section 5.2 presents a MIMO-OFDM model, infers statistical reciprocity, and describes estimation of the spatial covariance without any training overhead. Downlink optimization, including choice of antenna spacing, using this implicit covariance feedback is described in Section 5.3. Section 5.4 describes uplink optimization based on the spatial covariance estimate, using a novel noncoherent technique that provides beamforming gain without explicit estimation of the channel realization for each subcarrier. Section 5.5 provides our conclusions.

5.2 Modeling

We start with industry-standard statistical models for simulating outdoor space-time channels (Saleh and Valenzuela, 1987; Pedersen *et al.*, 1999). Such measurement-based models specify the power delay profile (PDP) and the power angle profile (PAP), as well as the distribution of the delays and the angles of arrival/departure of various multipath components. The PDP specifies the power distribution versus time, while the PAP specifies the power distribution as a function of the angle of arrival. A valid transceiver design must exhibit good performance at the nominal Signal-to-Noise Ratio (SNR) for "most" random channel realizations consistent with such a statistical model. For our information-theoretic investigation, we show that simulation-based statistical models can be replaced by bandwidth-dependent tap delay line (TDL) models that are more amenable to analytical insight.

5.2.1 Vector tap delay line channel model

We consider outdoor channels in which the base station (BS) is located high enough, and far enough away from the mobiles, that signals reaching a particular mobile leave the BS in a narrow spatial cone. As in the classic Saleh-Valenzuela model (Saleh and Valenzuela, 1987), the channel response is decomposed into clusters. Experimental measurements of outdoor channels (Pedersen *et al.*, 1999, 1997; Martin, 2002) indicate that the number of clusters is small, usually one or two. The power delay profile within each cluster is well modeled as exponential, and the power angle profile for each cluster as Laplacian. Thus, a "single cluster channel" would have an exponential PDP and a Laplacian PAP, while a "two cluster channel" would have a PDP comprised of the sum of two exponential profiles (each with a different start time, rate of decay, and total power), and a PAP comprised of the sum of two Laplacian profiles.

For a system bandwidth of W, the taps in a TDL channel model are spaced apart by $1/W$. Assuming a large enough number of paths, each such tap is composed of a number of unresolvable taps. The phases of the unresolvable taps are well modeled as independent and identically distributed (i.i.d.), and uniformly distributed over $[0, 2\pi]$. This is because small changes in delay produce large changes in carrier phase, under the standard assumption that the carrier frequency is much larger than the signal bandwidth. Application of the central limit theorem now leads to the classical Rayleigh fading model, in which the resolvable taps are modeled as zero mean, circular Gaussian. The variance of these resolvable taps is the sum of strengths of the unresolvable constituent taps, and therefore depends on the power-delay profile, $P_\tau(\cdot)$. For a multiantenna system, the channels seen by different antenna elements are modeled as correlated and jointly complex Gaussian, again applying the central limit theorem.

As an example, consider a MISO channel modeling a typical downlink. Letting $P_\tau(\cdot)$ and $P_\Omega(\cdot)$ denote the channel power delay profile and power angle profile, respectively, we obtain the following vector TDL model (ignoring the effect of channel time variations):

$$\mathbf{h}_W(\tau) = \sum_{l=0}^{\infty} A_l \mathbf{v}_l \delta(\tau - \frac{l}{W}) \tag{5.1}$$

where we set

$$A_l \propto \sqrt{P_\tau(\frac{l}{W})}, \quad l = 0, \ldots, \infty \tag{5.2}$$

to capture the dependence of tap strength on PDP, and where the i.i.d. complex Gaussian vectors $\mathbf{v}_l \sim \mathcal{CN}(0, \mathbf{C})$, with the spatial covariance matrix $\mathbf{C}$ determined by the array manifold and the channel PAP. Specifically, the spatial covariance is given by

$$\mathbf{C} = E[\mathbf{a}(\Omega)\mathbf{a}(\Omega)^H] = \int_{-\pi}^{\pi} \mathbf{a}(\Omega')\mathbf{a}(\Omega')^H P_\Omega(\Omega')d\Omega' \tag{5.3}$$

where $\mathbf{a}(\Omega)$ is the base station array response as a function of angle of departure Ω. As a running example, we consider a linear array, for which

$$\mathbf{a} = [a_1 \ldots a_{N_T}]^T, \quad a_l(\Omega) = e^{j(l-1)2\pi\frac{d}{\lambda}sin(\Omega)}, \quad l = 1, \ldots, N_T \tag{5.4}$$

where d is the antenna array spacing, and λ the carrier wavelength. N_T is the number of transmit antennas. This corresponds to a one dimensional equally spaced antenna array with spacing d.

If the mobile has multiple antennas, then, assuming that there is sufficiently rich scattering around the mobile, the channels from the BS to the different mobile antennas are well modeled as i.i.d. realizations of the preceding MISO model.

5.2.2 Spatial covariance estimation from uplink measurements

We first observe that uplink measurements can be employed to estimate the spatial covariance matrix $\mathbf{C}$. For simplicity of notation, we assume in the following that the mobile has one antenna, and communicates with a BS with an N element antenna array. Since the responses from the base station array to different antenna elements at the mobile are modeled as i.i.d., more mobile antennas would provide even more averaging when estimating the covariance matrix on the uplink.

The mobile employs K subcarriers (which may not be contiguous), and the received signal vector on the k^{th} subcarrier is given by

$$\mathbf{s}_k = \mathbf{h}_k x_k + \mathbf{n}_k, \tag{5.5}$$

where $\mathbf{h}_k$ is the $N \times 1$ channel frequency response, $\mathbf{n}_k$ is AWGN with

$E[\mathbf{n}_j \mathbf{n}_k^H] = 2\sigma^2 \delta_{jk} \mathbf{I}_N$, and $\mathbf{I}_N$ denotes the $N \times N$ identity matrix. We know from Section 5.2.1 that the $\mathbf{h}_k$ are identically distributed, with $\mathbf{h}_k \sim \mathcal{CN}(0, \mathbf{C})$.

A spectral decomposition of the channel covariance yields

$$\mathbf{C} = \mathbf{U}\mathbf{\Lambda}\mathbf{U}^H, \tag{5.6}$$

where the eigenvector matrix $\mathbf{U} = [\mathbf{u}_1 \ldots \mathbf{u}_N]$ is unitary, and $\mathbf{\Lambda}$ is diagonal with eigenvalues $\{\lambda_l\}$ arranged in decreasing order. The eigenvalue λ_l represents the strength of the channel on l^{th} eigenmode $\mathbf{u}_l$.

For the large delay spreads typical of outdoor environments, the coherence bandwidth is small, and the correlation between the channel responses at different frequencies dies out quickly with their separation. Thus, the base station can accurately estimate $\mathbf{C}$ by measuring the channel over a rich enough set of frequencies on the uplink (Barriac and Madhow, 2003, 2004b). Averaging over frequency bins, the base station forms an empirical autocorrelation matrix $\mathbf{R}$:

$$\mathbf{R} = \frac{1}{K} \sum_{k=1}^{K} \mathbf{s}_k \mathbf{s}_k^H. \tag{5.7}$$

With $E[|x_k|^2] = 1$, it is easy to show that $\mathbf{R}$ is an estimate of $\mathbf{C} + 2\sigma^2 \mathbf{I}_N$, where σ^2 is the noise variance per dimension. Thus, if λ_l are the eigenvalues of $\mathbf{C}$, the eigenvalues of $\mathbf{R}$ are $\lambda_l + 2\sigma^2$. The eigenvectors of the two matrices are the same. An eigendecomposition of $\mathbf{R}$ therefore yields the dominant channel eigenmodes. Typically, the number of dominant eigenmodes is small for an outdoor channel because of the narrow PAP corresponding to signals received from a given mobile.

In the succeeding sections, we see how the preceding covariance estimate can be employed for both downlink and uplink optimization.

5.3 Downlink optimization with implicit covariance feedback

The empirical correlation matrix of the the uplink signal from a given mobile, as computed in Section 5.2.2, provides implicit feedback regarding the downlink covariance matrix from the BS to that mobile.

5.3.1 Shannon-theoretic performance evaluation

Once the spatial covariance matrix $\mathbf{C}$ is known with sufficient accuracy, downlink transmission for a system with N_T BS antennas and N_R mobile antennas ($N_T \gg N_R$) is optimized by sending i.i.d. Gaussian inputs for each subcarrier, so that the ergodic capacity is that of a narrowband system with covariance feedback, as considered in (Visotsky and Madhow, 2001; Jafar *et al.*, 2001). The optimal policy for each subcarrier is to send independent Gaussian inputs along the eigenvectors of $\mathbf{C}$, with the power allocated to each eigenmode determined by a waterfilling strategy. In practice, for an outdoor channel, the transmitted power can be concentrated along a small number K_T ($K_T \ll N_T$) of dominant eigenmodes using a linear precoding matrix, along with a space-time code designed for a virtual $K_T \times N_R$ MIMO system, in which the number K_T of virtual transmit antenna elements equals the number of eigenmodes with nonzero transmitted power. If λ_i is the eigenvalue for the ith eigenmode (in decreasing order) which is employed for transmission, and p_i is the power allocated to the ith eigenmode, then the mutual information along a given subcarrier is a random variable which can be written as

$$I(\mathbf{p}) = \log \left| \mathbf{I}_{N_R} + \frac{1}{\sigma_n^2} \sum_{i=1}^{K_T} \mathbf{z}_i \mathbf{z}_i^H p_i \lambda_i \right|, \tag{5.8}$$

where the $\mathbf{z}_i$ are independent $N_R \times 1$ vectors whose elements are i.i.d. $\mathcal{CN}(0,1)$, and σ_n^2 is the noise variance per dimension. We normalize the channel eigenvalues $\{\lambda_i\}$ such that $\sum_{i=1}^{N_T} \lambda_i = N_T$, and the powers such that $\sum_{i=1}^{K_T} p_i = P$.

We now discuss the Shannon-theoretic performance attained by the preceding strategy. For a MISO system employing multiple subcarriers on the downlink, spanning a bandwidth W, the spectral efficiency I_W, or the mutual information averaged across subcarriers, is given by averaging (5.8) across the subcarriers employed. Under mild conditions on the power delay profile, the channels seen by different subcarriers decorrelate rapidly enough that such averages obey a central limit theorem. The spectral efficiency is therefore well modeled as Gaussian, with mean given by the expectation of (5.8). This is simply the ergodic capacity of a single subcarrier, given by

$$E[I_W] = E[I(\mathbf{p})]. \tag{5.9}$$

For a single cluster channel, the variance of the spectral efficiency can be estimated as follows (Barriac and Madhow, 2004a):

$$var[I_W] \approx \frac{N_R \sum_{i=1}^{K_T} (\lambda_i p_i)^2}{(1 + \sum_{i=1}^{K_T} \lambda_i p_i)^2} \frac{1}{W} \int P^2(\tau)\, d\tau, \tag{5.10}$$

where the PDP is normalized as $\int P(\tau) d\tau = 1$. Note that the variance is inversely proportional to the system bandwidth.

Knowing the mean and variance of the spectral efficiency, we can now provide simple analytical estimates of the outage rate based on the Gaussian approximation. Let rate $R(\epsilon)$, which is defined to be the largest transmission rate R (normalized by the system bandwidth W), such that the following condition holds:

$$P[I_W \leq R] \leq \epsilon. \tag{5.11}$$

Modeling I_W as Gaussian, we obtain the following approximation for $R(\epsilon)$,

$$\hat{R}(\epsilon) \approx E[I_W] - \sqrt{var[I_W]} * Q^{-1}(\epsilon), \tag{5.12}$$

where $Q(x)$ is the complementary cumulative distribution function of a standard Gaussian random variable. The absolute outage rate, of course, is given by $R(\epsilon)W$.

From (5.10), we note that the variance of I_W decreases with increasing W, regardless of the power allocation across eigenmodes. Thus, for large system bandwidths, the outage rate is approximately maximized by maximizing the ergodic capacity $E[I_W]$. We will refer to this observation later, when we discuss downlink optimization by varying antenna spacing.

5.3.2 Accuracy of implicit covariance feedback

There are two key issues affecting the accuracy of estimating the covariance matrix $\mathbf{C}$ as in the previous section:
(i) The covariance must vary slowly enough such that, when the base station sends to user k, the estimate $\hat{\mathbf{C}}_k$ is still valid.
(ii) A mobile must employ enough subcarriers, and a wide enough separation among the subcarriers, that the empirical average (5.7) provides an accurate covariance estimate.

Both of these conditions are met for a wide variety of resource sharing models, including FDD systems where the uplink and downlink are contiguous (Barriac and Madhow, 2004b). As an example, we consider a TDD system with TDMA on the uplink and TDM on the downlink, which implies that there is a significant delay between acquiring covariance feedback based on uplink measurements, and employing it on the downlink.

We assume an OFDM system with 1024 subcarriers spaced 25 KHz apart. The PAP is initially $L(0^\circ, 5^\circ)$ ($L(M, \alpha)$ denotes a Laplacian distribution with mean M and variance $2\alpha^2$) and the PDP is exponential with an rms value of 0.5 μs. SNR is set to 10 dB. The BS has 6 antennas, with a typical antenna spacing of $d/\lambda = 0.5$. At this spacing, beamforming is the optimal transmit strategy for the given PAP.

The TDD system under consideration is shown in Fig. 5.1. Each user sends

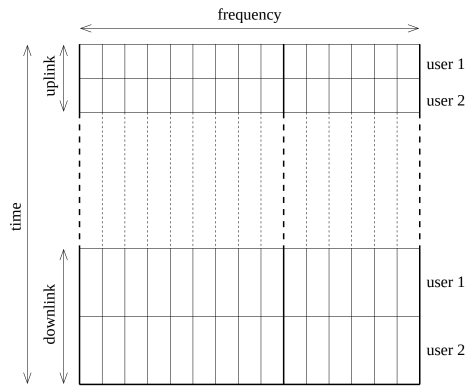

Fig. 5.1. A TDD system with TDMA on the uplink and TDM on the downlink

to the base station using the entire frequency band for a certain amount of time, and subsequently the base station takes turns sending to the mobiles over whole band. For such a system, K in (5.7) equals the entire set of frequency bins for all users. If the bandwidth is large, $\hat{\mathbf{C}}_k$ is clearly a good approximation for $\mathbf{C}_k$, but the question remains as to whether this covariance will remain valid until the BS is ready to reply to that mobile on the downlink. The longest a user will have to wait until it hears back from the BS is approximately the number of users in the system multiplied by the time the BS sends to each user. For a rate of 20 Mbps and 10 packet payloads of 10 000 bits each, the time the BS sends to each mobile is approximately 5 msec. If there are 10 users, this means the total delay is around 50 msec. However, even if the channel is fast fading, the covariance need not change much in this length of time, since it depends only on the power-angle profile, which in general is slowly varying. It is shown in Nicoli *et al.* (2002) that for a mobile 500 m from the base station traveling less than 1000 km/h, and a BS station with 8 antennas spaced half a wavelength apart, the channel statistics can be considered stationary for around 100 msec. Thus, the PAP, and hence the covariance would also be stationary for that time length.

We now consider how variations (we can assume they are small) in the PAP would affect system performance. For a mobile moving away from the BS at 100 km/h, the angle between the BS and the mobile will change approximately $0.08°$ in 50 msec. If the center angle of the PAP changes a corresponding amount, we would like to know how this impacts performance results. Table 5.1 gives the 1% outage rate and ergodic capacity of a wideband system when the actual PAP differs for the PAP used to estimate the covariance. The outage rates are computed using the transmit strategy

Actual PAP	Feedback PAP	C	R_o
$\Omega \sim L(0.0°, 5°)$	no feedback	3.12	2.70
$\Omega \sim L(0.0°, 5°)$	$\Omega \sim L(0.0°, 5°)$	4.83	4.13
$\Omega \sim L(0.6°, 5°)$	$\Omega \sim L(0.0°, 5°)$	4.83	4.14
$\Omega \sim L(2.9°, 5°)$	$\Omega \sim L(0.0°, 5°)$	4.76	4.09
$\Omega \sim L(0.0°, 9°)$	$\Omega \sim L(0.0°, 5°)$	4.83	4.13
$\Omega \sim L(0.0°, 1°)$	$\Omega \sim L(0.0°, 5°)$	4.82	4.13
$\Omega \sim L(2.9°, 9°)$	$\Omega \sim L(0.0°, 5°)$	4.77	4.10
$\Omega \sim L(2.9°, 1°)$	$\Omega \sim L(0.0°, 5°)$	4.76	4.08

Table 5.1. *The ergodic capacity (C) and 1% outage rate (R_o) in b/sHz when the BS station beamforms to the dominant eigenmode of $\hat{\mathbf{C}}_k$, computed for $\Omega \sim L(0°, 5°)$.*

that maximizes ergodic capacity. It is assumed that the power angle profile remains Laplacian, and that only the mean and/or angular spread change with time. The first row shows the capacity and outage rate when there is no feedback and the transmitter employs a full blown space-time code (the optimal transmit strategy when no feedback is available). The second row shows the capacity and outage rate when the BS has perfect covariance feedback information and beamforms in the direction of the covariance's dominant eigenmode (beamforming is the optimal strategy in this scenario for the given parameters). The following rows display the resulting capacity when the BS beamforms using imperfect covariance information. It can be seen that even if the base station uses covariance information obtained from a Laplacian whose mean has since shifted 2.9°, and whose variance has doubled, deleterious effects on performance are minimal. Even in this case, where the changes in the PAP are much larger than one might expect, both the ergodic capacity and outage rate are much higher than the corresponding quantities when no feedback is available.

5.3.3 Optimal antenna spacing

We have seen that the spatial covariance depends on the PAP and the array manifold, with the latter determined by the array geometry. Now that we know that covariance feedback is readily available, a natural question to ask is the following: how should we choose the antenna array geometry so as to optimize performance? When there is no feedback, a reasonable strategy is to send i.i.d. Gaussian input from each transmit antenna, and the best performance is attained by spacing the antennas far enough apart that they see uncorrelated responses (Barriac and Madhow, 2004a). However, when the BS knows the channel covariance, the optimal antenna spacing is expected to be much smaller. For example, if we plan to beamform along the dominant eigenmode, then it makes sense to space the antennas such that the eigenvalue of this eigenmode is maximized.

We will focus on optimizing antenna spacing so as to maximize ergodic capacity (assuming optimal transmission with covariance feedback). As we have seen in Section 5.2.2, for large enough system bandwidth, this also approximately maximizes the outage rate. Maximization of ergodic capacity can be achieved by considering a single subcarrier, since the expected mutual information achieved by a given strategy is the same across subcarriers. From (5.8), the ergodic capacity with optimal power allocation is given by

$$C = \max_{p_i : \sum_{i=1}^{N_T} p_i = P, p_i \geq 0} E\left[\log\left|\mathbf{I}_2 + \frac{1}{\sigma_n^2}\sum_{i=1}^{N_T} \mathbf{z}_i \mathbf{z}_i^H p_i \lambda_i\right|\right], \tag{5.13}$$

where the $\mathbf{z}_i$ are independent $N_R \times 1$ vectors whose elements are i.i.d. $\mathcal{CN}(0,1)$.

Ideally, we would like to maximize C by optimizing the antenna spacing, given the PAP and the SNR. This problem is difficult to solve because the eigenvalues $\{\lambda_i\}$ capacity depends in a complex fashion on the PAP and the array geometry. We therefore consider a simplified thought experiment, in which we consider a system with K eigenmodes with equal nonzero eigenvalues, with the remaining eigenmodes corresponding to zero eigenvalues. The question then becomes: what is the optimal value $K = K_{opt}$, as a function of the number of receive elements N_R, and the SNR. The results of such a thought experiment provides valuable guidance on antenna spacing, even though it may not always be possible to implement its prescriptions. For example, for $K_{opt} = 1$, we should space the antennas closely enough to create a single dominant eigenmode. However, if there are two multiple clusters with very different angles of departure from the BS, then there will be two dominant eigenmodes for any reasonable value of antenna spacing.

The results of the thought experiment can be paraphrased as follows: create a number of eigenmodes that is roughly equal to the number of receive elements N_R (except at very low SNR, where the optimal number of

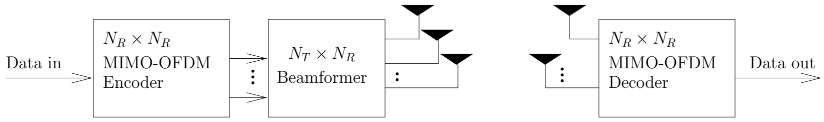

Fig. 5.2. MIMO-OFDM system with beamforming, where the number of transmit elements $N_T = N_b$, and the number of receive elements $N_R = N_s$.

eigenmodes is one).† Beamforming along these eigenmodes therefore creates an effective $N_s \times N_s$ MIMO system. While beamforming gains can be increased by increasing the number N_T of antennas at the BS transmitter, the complexity of OFDM processing at the transmitter scales as N_R, the much smaller number of antennas in the mobile receiver, since the beamforming weights are independent of the subcarriers. See Fig. 5.2. More importantly, the receiver in the subscriber unit only sees the effective $N_R \times N_R$ MIMO system, so that downlink performance can be improved by scaling up N_T, without any additional burden on the less capable receiver in the subscriber unit.

From a practical viewpoint, it is usually possible to space the transmit antennas so as to roughly follow the prescriptions of the thought experiment: in general, it is *not* possible to make the eigenvalues of the dominant eigenmodes equal, but spacing the antennas such that the number of dominant modes is close to K_{opt} still gives large capacity gains, as demonstrated in the following example. Consider a BS with 6 antennas transmitting to a mobile whose PAP is $L(0°, 5°)$. The SNR, P/σ_n^2, is set to 10 dB. As the antenna spacing changes, so does $\mathbf{\Lambda}$, and hence the optimal values of p_i, which can be solved for numerically. Fig. 5.3a shows how the ergodic capacity changes for different values of d/λ (the antenna spacing over the wavelength). At $d/\lambda = 8$, all channel eigenvalues are equal and hence the capacity at this point corresponds to the maximum capacity attainable when there is no feedback. As d/λ decreases, the channel energy becomes concentrated in fewer eigenmodes, until only one eigenmode is dominant. Below $d/\lambda = 0.5$, beamforming is optimal. (See Jafar and Goldsmith (2001) for the necessary and sufficient conditions for the optimality of beamforming.) We do not consider values of d/λ smaller than 0.4 because at very close spacing, the different antennas can no longer be treated as separate elements due to electro-magnetic coupling.

It is evident that beamforming with the BS antennas spaced at 0.4λ is superior to using a full blown space time code with $d/\lambda = 8$, giving a gain

† See Barriac and Madhow (2004b) for details and caveats. Also see Boche and Jorswieck (2003a) for results for $N_R = 1$.

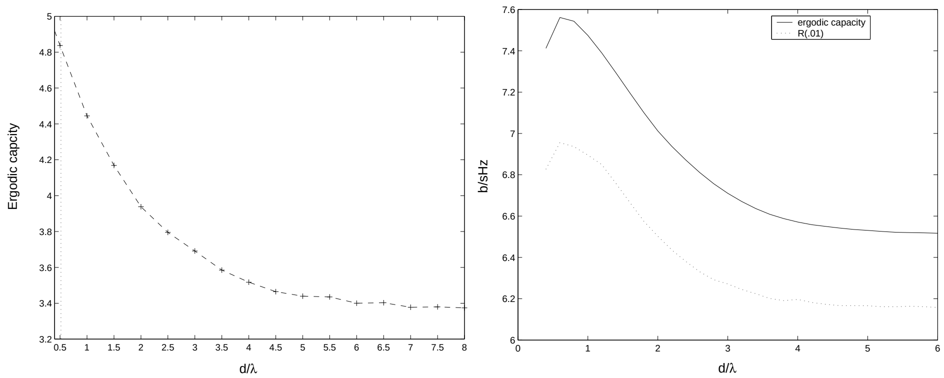

(a) $N_R = 1$: To the left of the dotted line, beamforming is optimal.

(b) $N_R = 2$ and $\tau_{rms} = 0.5$ μs, with 1% outage rate.

Fig. 5.3. Ergodic capacity vs. d/λ when $N_T = 6$ and $\Omega \sim L(0°, 5°)$.

of over 1.5 b/sHz. Not only is capacity increased by using a smaller spacing, but complexity is decreased dramatically by using beamforming instead of space-time codes.

Now, suppose that there are two receive elements. Noting that $K_{opt} = 2$ when $N_R = 2$ at moderate SNR, we expect that spacing the antennas such that there are two dominant eigenmodes should give the best performance. Again, we consider $N_T = 6$ and the PAP$\sim L(0°, 5°)$, but with N_R now equal to 2. For different values of d, the optimal powers p_i are calculated numerically by approximating derivatives by differentials and using the projected gradient descent algorithm. Values for the ergodic capacity are plotted vs. d/λ in Fig. 5.3b. Below $d/\lambda = 0.82$, sending along 2 eigenmodes is optimal. As expected, the maximum capacity occurs when 2 eigenmodes are dominant, at $d/\lambda = 0.7$. We also plot the outage rate in the figure, assuming that there are 1024 subcarriers spaced 25 KHz apart, and that the PDP is exponential with an rms delay spread of 0.5 μs. As expected from the discussion in Section 5.2.2, the antenna spacing that maximizes ergodic capacity also roughly maximizes the outage rate.

5.4 Uplink optimization using noncoherent eigenbeamforming

In this section we discuss how implicit knowledge of the channel covariance at the BS can be used with noncoherent demodulation on the *uplink*, even when no other channel information is available. The complexity remains

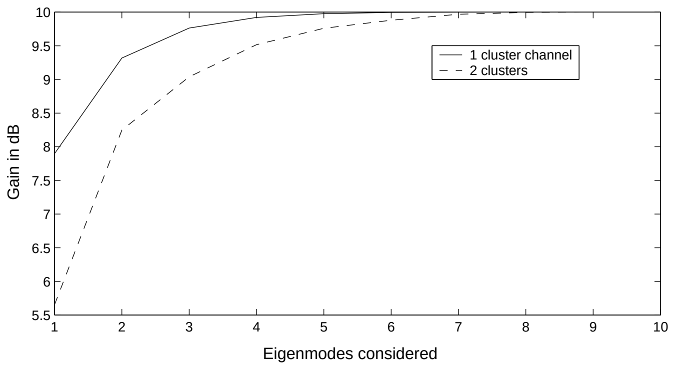

Fig. 5.4. Eigenbeamforming gain over a single antenna receiver

practicable even as the receiver (BS) enjoys an SNR advantage from scaling up the number of antennas. Noncoherent communication is well-suited to the uplink of a cellular system in which the base-station must estimate a time-varying channel to each mobile. Pilot-symbol based channel estimation is potentially more efficient on the downlink, since the mobiles are able to share a common pilot channel. Accurate estimates of the spatial covariance matrix, available through averaging in wideband systems, allow eigenbeamforming (Jacobsen *et al.*, 2004) at the receiver along the dominant channel modes. For a typical outdoor channel, where the number of dominant modes is small, this allows the receiver to increase its SNR by scaling up the number of antennas, while limiting the demodulation and decoding complexity which scales with the number of channel modes used by the receiver.

Once the channel covariance is obtained at the BS by averaging uplink measurements the BS will project the received signal along the L dominant eigenvectors of the covariance matrix, obtained from its factorization (5.6). This yields L parallel uncorrelated OFDM channels $\{\langle \mathbf{s}, \mathbf{u}_l \rangle\}_{l=1}^{L}$, where $\mathbf{s}$ denotes the $N_b \times 1$ received signal, as in (5.5), and L is typically much smaller than the number of antenna elements N_b. As a rough measure of the performance gain relative to a single antenna system, we define *beamforming gain* as the SNR if the signal power is summed over the L chosen eigenmodes, relative to the SNR for a single antenna element. This yields the following formula for the beamforming gain as a function of L:

$$G(L) = 10 \log_{10} \left(\frac{N_b \sum_{l=1}^{L} \lambda_l}{\sum_{l=1}^{N_b} \lambda_l} \right), \tag{5.14}$$

where λ_l are the channel eigenvalues.

Fig. 5.4 shows the beamforming gain as a function of the number of eigenmodes used for a 10 antenna system. The upper curve is for a single cluster channel whose power angle profile is Laplacian with zero mean and angular spread $10°$, where angular spread is defined as the variance of Ω. The lower plot is for a two cluster channel where the first cluster's power angle profile is as above, and the second cluster's power angle profile is also Laplacian with angular spread $10°$, but has its mean at $45°$ (both clusters with the same power). The total receive power is normalized to be the same for both plots. Note that beamforming gain quickly plateaus as a function of L. Thus, beamforming along the dominant eigenmode captures most of the received energy for the one cluster channel, while using the first two eigenmodes captures most of the energy in the two cluster channel. Thus, for typical outdoor channels, estimation of the channel covariance enables the use of a small number of eigenmodes by the demodulator and decoder, limiting complexity while preserving the SNR advantage from scaling up the number of receive elements.

The signals for the L eigenmodes can be combined in a number of ways. The gain on the kth subcarrier along the lth eigenmode is given by $g_k(l) = \langle \mathbf{h}_k, \mathbf{u}_l \rangle$. One possibility is to explicitly estimate the scalar channel gains $\{g_k(l), l = 1, \dots, L\}$ using pilots, and to then perform coherent diversity combining of the L branches to obtain an estimate of x_k. The advantage that this may have over estimation of the original $N_b \times 1$ channel vector $\mathbf{h}_k$ is that fewer gains may need to be explicitly estimated. Another possibility is noncoherent diversity combining, which is consistent with the goal of reducing overhead in uplink transmission. In Jacobsen *et al.* (2004), serial concatenation of an outer binary channel code with an inner differential modulation code is employed for approaching noncoherent capacity on the uplink of a wideband cellular channel. A simple, yet effective combining strategy with iterative noncoherent processing is used: Parallel noncoherent demodulators with extrinsic information from the channel decoder process L dominant channel modes. The soft outputs of the demodulators are then combined and sent back to the decoder as priors, setting up the next round of parallel demodulation and decoding.

In addition to beamforming gain, various levels of diversity are attained by processing the channel modes in parallel. Fig. 5.5 shows the affect of diversity level on noncoherent capacity when the received power is normalized to one and distributed equally amongst $L = 1, 2, 3, 4$ dominant eigenmodes. To illustrate beamforming gain in this context, consider a 10 element BS array with one dominant channel mode. The SNR per antenna element in such a system is 10 dB less than that of a single antenna system operating

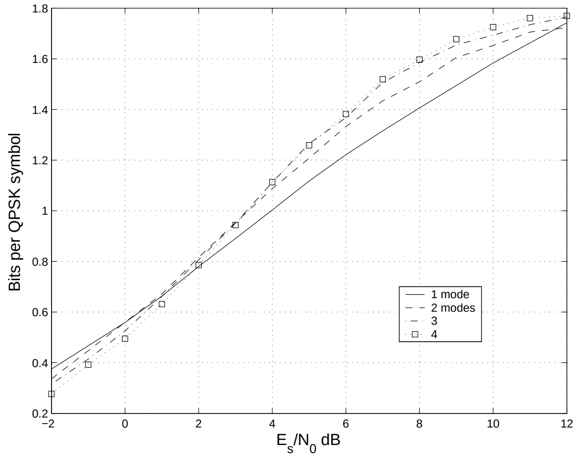

Fig. 5.5. Noncoherent block fading capacity with varying number of dominant, equal-strength eigenmodes

at the same rate; for example, we see from Fig. 5.5 that a single antenna system requires SNR of 2 dB for a spectral efficiency of 0.8 bits/symbol; the corresponding SNR per antenna element for a 10 element array with a single dominant mode is -8 dB.

5.5 Conclusions

Space-time communication systems that leverage uplink/downlink asymmetry in addition to statistical reciprocity inherent to wideband outdoor channels enjoy large performance gains, while at the same time reducing signal processing complexity at both the base station and mobile radio. Specifically, the techniques presented in this chapter enable an increase in capacity by increasing the number of antennas at the base station, without *any* impact on transceiver complexity at the mobile. While the performance gains from these techniques are evaluated in Shannon theoretic terms, advances in turbo-like coded modulation imply that these information theoretic limits are achievable at reasonable complexity.

References

Barriac, G. and Madhow, U. (2003). Wideband space-time communication with implicit channel feedback. In *Seventh International Symposium on Signal Processing and its Applications*.

—— (2004a). Characterizing outage rates for space-time communication over wideband channels. *IEEE Trans. Commun.*, **52** (12), 2198–2208.

—— (2004b). Space-time communication for OFDM with implicit channel feedback. *IEEE Trans. Inform. Theory*, **50** (12), 3111–3129.

Biglieri, E., Caire, G., and Taricco, G. (2001). Limiting performance of block-fading channels with multiple antennas. *IEEE Trans. Inform. Theory*, **47** (4), 1273–1289.

Boche, H. and Jorswieck, E. (2003a). Optimum power allocation, and complete characterization of the impact of correlation on the capacity of MISO systems with different CSI at the transmitter. In *IEEE International Symposium of Information Theory*.

—— (2003b). Optimum power allocation for MISO systems, and complete characterization of the impact of correlation on the capacity. In *International Conference on Acoustics, Speech, and Signal Processing*, vol. 4, 373–376.

Cavers, J. (2002). Single-user and multiuser adaptive maximal ratio transmission for Rayleigh channels. *IEEE Trans. Veh. Technol.*, **49** (6), 2043–2050.

Hochwald, B. and Marzetta, T. (2001). Adapting a downlink array form uplink measurements. *IEEE Trans. Signal Processing*, **49** (3), 642–653.

Jacobsen, N., Barriac, G., and Madhow, U. (2004). Noncoherent eigenbeamforming for a wideband cellular uplink. In *IEEE International Symposium on Information Theory*.

Jafar, S. and Goldsmith, A. (2001). On optimality of beamforming for multiple antenna systems with imperfect feedback. In *IEEE International Symposium of Information Theory*.

Jafar, S., Vishwanath, S., and Goldsmith, A. (2001). Channel capacity and beamforming for multiple transmit and receive antennas with covariance feedback. In *IEEE Conference on Communication*.

Jongren, G., Skoglund, M., and Ottersten, B. (2002). Combining beamforming and orthogonal space-time block coding. *IEEE Trans. Inform. Theory*, **48** (3), 611–627.

Kang, M. and Alouini, M. (2003). Water-filling capacity and beamforming performance of MIMO systems with covariance feedback. In *IEEE Workshop on Signal Processing*, 556–560.

Lau, K., Liu, Y., and Chen, T. (2003). Optimal partial feedback design for MIMO block fading channels with causal noiseless feedback. In *IEEE International Symposium on Information Theory*, 65.

Liang, Y. and Chin, F. (2001). Downlink channel covariance matrix estimation and its applications in wireless DS-CDMA systems. *IEEE J. Select. Areas Commun.*, **19** (2), 222–232.

Martin, U. (2002). A directional radio channel model for densely built up urban areas. In *Proc. 2nd EMPCC*, 237–244.

Medles, A., Visuri, S., and Slock, D. (2003). On MIMO capacity for various types of partial channel knowledge at the transmitter. In *Proc. IEEE Information Theory Workshop*, 99–102.

Morgan, D. (2003). Downlink adaptive array algorithms for cellular mobile communications. *IEEE Trans. Commun.*, **51** (3), 476–488.

Mukkavilli, K., Sabharwal, A., and Erkip, E. (2003a). Beamformer design with feedback rate constraints: criteria and constructions. In *IEEE International Symposium on Information Theory*, 414.

Mukkavilli, K., Sabharwal, A., Erkip, E., and Aazhang, B. (2003b). On beamforming with finite rate feedback in multiple-antenna systems. *IEEE Trans. Inform. Theory*, **49** (10), 2562–2579.

Narula, A., Lopez, M., Trott, D., and Wornell, G. (1998). Efficient use of side information in multiple antenna data transmission over fading channels. *IEEE J. Select. Areas Commun.*, **16** (8), 1423–1435.

Nicoli, M., Simeone, O., and Spagnolini, U. (2002). Multislot estimation of fast-varying space-time channels in TD-CDMA systems. *IEEE Commun. Lett.*, **6** (9), 376–378.

Pedersen, K., Mogensen, P., and Fleury, B. H. (1997). Power-azimuth spectrum in outdoor environments. *IEEE Electronics Letters*, **33** (18), 1583–84.

—— (1999). Dual-polarized model of outdoor propagation environments for adaptive antennas. In *IEEE 49th Vehicular Technology Conference*, vol. 2, 990–5.

Raleigh, G. and Jones, V. (1997). Adaptive antenna transmission for frequency duplex digital wireless communication. In *Proc. IEEE International Conference on Communications*, vol. 6, 641–646.

Saleh, A. and Valenzuela, R. (1987). A statistical model for indoor multi-path propagation. *IEEE J. Select. Areas Commun.*, **5** (2), 128–137.

Simeone, O. and Spagnolini, U. (2003). Combined linear pre-equalization and BLAST equalization with channel correlation feedback. *IEEE Commun. Lett.*, **7** (10), 2663–2667.

Simon, S. and Moustakas, A. (2002). Optimizing MIMO antenna systems with channel covariance feedback. In *Bell Labs Technical Memorandum*.

Telatar, E. (1995). Capacity of multi-antenna Gaussian channels. *AT&T Bell Labs Internal Tech. Memo # BL0112170-950615-07TM.*

Visotsky, E. and Madhow, U. (2001). Space-time transmit precoding with imperfect channel feedback. *IEEE Trans. Inform. Theory*, **47** (6), 2632–2639.

Vook, F., Thomas, T., and Zhuang, X. (2003). Transmit diversity and transmit adaptive arrays for broadband mobile OFDM systems. In *Proc. IEEE Wireless Communications and Networking Conference*, vol. 1, 44–49.

Xia, P., Zhou, S., and Giannakis, G. (2004). Adaptive MIMO OFDM based on partial channel state information. *IEEE Trans. Signal Processing*, **52** (1), 202–213.

Zhou, S. and Giannakis, G. (2003). Optimal transmitter eigen-beamforming and space-time block coding based on channel correlations. *IEEE Trans. Inform. Theory*, **49** (7), 1673–1690.

Part II

Space-time modulation and coding

Part III

Receiver algorithms and parameter estimation

Part IV

System-level issues of multiantenna systems

Part V

Implementations, measurements, prototypes, and standards

Author index

Index